

# Analysis and design of the biasing network for 1 GHz bandwidth RF power amplifier

Md. Golam Sadeque<sup>1</sup>, Zubaida Yusoff<sup>2</sup>, Mardeni Roslee<sup>3</sup>, Shaiful Jahari Hashim<sup>4</sup>,  
Azah Syafiah Mohd Marzuki<sup>5</sup>

<sup>1,2,3</sup>Faculty of Engineering, Multimedia University, Selangor, Malaysia

<sup>4</sup>Faculty of Engineering, University Putra Malaysia, Selangor, Malaysia

<sup>5</sup>TM R&D Sdn Bhd, Selangor, Malaysia

## Article Info

### Article history:

Received Aug 29, 2020

Revised Jul 28, 2021

Accepted Aug 4, 2021

### Keywords:

Biasing network  
Open-circuit stub  
Quarter wave  
Radial stub  
Wideband

## ABSTRACT

The bandwidth of the wireless communication has increased due to the various applications of the wireless devices. A radio frequency power amplifier (RFPA) is one of the crucial components of the transceiver. So, to meet the requirement of the bandwidth, wideband RFPA is needed. The RFPA not only requires a wideband matching network but importantly the biasing network. For the next-generation communication system, a wideband biasing network is needed to operate in the wide GHz bandwidth range. In this paper, a wideband biasing network for the power amplifier is designed using a quarter-wave transmission line and a butterfly stub for the frequency band of 3.3 GHz to 4.3 GHz. Roger's RO3006 is used as the substrate for the design of the biasing network. The designed network performed well in the required frequency range. The performances of the biasing network have shown 9 dB to 19 dB return loss, the radio frequency (RF) isolation has more than 35 dB, and 0 dB to 1.5 dB insertion loss. This wideband biasing network can be used for the next generation communication system.

*This is an open access article under the [CC BY-SA](https://creativecommons.org/licenses/by-sa/4.0/) license.*



## Corresponding Author:

Zubaida Yusoff

Faculty of Engineering, Multimedia University

Cyberjaya Campus, Persiaran Multimedia, Cyberjaya, Selangor, Malaysia

Email: [zubaida@mmu.edu.my](mailto:zubaida@mmu.edu.my)

## 1. INTRODUCTION

The use of wireless communication systems is increasing day by day in many applications such as cellular phones, wireless local area networks (WLAN), broadcasting, and wireless computer peripherals to be part of our daily lives. Radio frequency power amplifiers (RFPA) are the essential components of the wireless communication system. RFPA consumes dendritic cells (DC) power to boost up the input signal to deliver with maximum output power at RF frequency. The RFPAs are the most costly component at the front end [1]. So, high efficiency is a key requirement of RFPA design. A high efficient RFPA leads to low power consumption, smaller battery size, and lessen the cooling requirement [2]. The RFPA consist of mainly four components. These components are the biasing network, stability network, input matching network (IMN), and output matching network (OMN). Due to the large bandwidth requirement, the wideband power amplifier is needed for the next-generation communication (5G) system with good performances. To increase the performances of RFPA, scientists all over the world are working on the different parts of the RFPA. The design of the biasing network is one of them. Various configuration and techniques have been developed and explored for the biasing network. The function of the biasing network is to offer high impedance at the RF frequency signal while offering minimum resistance to DC.

Different types of biasing networks have been designed to meet the requirement of the frequency band. At the low-frequency band, resistors and inductors are used as a biasing network [3], [4], but at the high frequency, the biasing network is designed using a large inductor and the quarter-wave microstrip line (QWML) [5], [6]. In some cases, QWML is combined with the quarter-wave open circuit stub (QWOS) or radial stub [7], [8]. The frequency of operation of RFPA is different for different applications. The upcoming 5G communication system will operate mainly in two frequencies region, namely low-frequency (below 6 GHz) and high-frequency (above 6 GHz) [9]. In the low-frequency region, many countries will operate at a different frequency band below 6 GHz. Some countries will operate in the frequency band ranges from 3.3 GHz to 4.2 GHz [10], [11].

In this paper, a wideband biasing network is presented for 1 GHz bandwidth RFPA for the frequency range of 3.3 GHz to 4.3 GHz. The proposed biasing network is designed using the QWML and the butterfly stub. This paper is organized as follows; section 2 briefly describes the latest work related to the biasing network. Section 3 presents the design methodology of the wideband biasing network for the RFPA. The performances of the RFPA are described in section 4. Finally, the conclusion is drawn in section 5.

## 2. LITERATURE REVIEW

The RFPA are used in every communication system, and so their characteristics are crucial for the efficiency of the communication system. The basic components of the RFPA are shown in Figure 1. The procedure of biasing the active device can be divided into two steps; selection of the biasing operating (quiescent) point and the biasing network design. Firstly, the biasing point is selected based on the type of power amplifier and the targeted performance such as the efficiency and the output power. The second step is to select the biasing scheme by considering the cost, bandwidth, and distortion. The structure of the biasing network depends on the frequency of operation. At a very low frequency, the biasing voltage can be applied directly to or through a resistor at the biasing point, but at the high frequency, the biasing is more complex and cannot be applied directly [3]. The commonly used methods of transistor biasing at low frequency are; the base resistor method, the collector to base bias method, the biasing with the collector feedback resistor, and the voltage-divider bias method [12]. At high frequency, to improve the performances of the RFPA, two types of biasing network are used; fixed biasing and dynamic biasing [13]. In terms of efficiency, the dynamic biasing performs better.

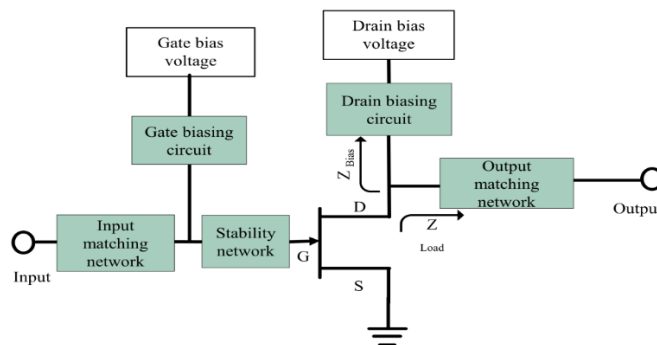


Figure 1. Block diagram of the RFPA

The structure of the biasing network is a tradeoff among stability, linearity, and complexity. A conventional biasing network at low and medium frequency consists of a resistor at the gate and an inductor at the drain [4], but at the high frequency, the QWML is preferable [6]. The biasing resistors and inductors are shorted for the RF signal at the DC biasing point through the bypass capacitors, as shown in Figure 2(a). As an example, 4310LC wideband bias chokes are selected for the PA design to block RF signal at the biasing [14], [15]. The gate and drain biasing structure are the same except that sometimes a resistor is added to the gate to increase the stability. At the biasing tee, the different valued capacitors are also added as bypass capacitors. Yang *et al.* [6] showed that the  $\lambda/4$  transmission line could be used as a biasing network both at the drain and the gate. This biasing network is used for the frequency range of 1.15 GHz to 2.2 GHz. At the end of the quarter-wave transmission line, the microstrip line of an arbitrary width is added for soldering the bypass capacitors and the biasing voltage source, as shown in Figure 2(b), it is assumed that the QWML is perfectly short-circuited at the end of the line through the capacitor. But practically, the capacitor that has low resistance will not perfectly short the RF signal. As a result, the QWML is not perfectly open at the RF signal at the biasing tee. To overcome this problem, the biasing network is designed using the QWML and

the radial stub at the end of the QWML [5], [7], [16]. The radial stub will create short circuit at the connected point. The QWML will transfer short to open circuit at the biasing tee.

Ultra-wideband biasing network is designed using the distributed high pass and bandpass network [17]. It is seen that the biasing tee consists of a high pass circuit that performs better compared to the bandpass network. This circuit works well for the ultra-wideband but it is more complex and can cause more insertion loss.

The bandstop filter can also be used as a biasing network to block the RF signal while maintaining the perfect transmission for the DC. The order of the bandstop filter depends on the frequency and bandwidth of the RF signal [18]. But due to the complex structure, the bandstop filter cannot be used as a biasing choke because it will affect the performances of the RFPA. Therefore, a simple bandstop filter is designed using the quarter-wave microstrip line, and a radial stub as a biasing choke [7], [19] is shown in Figure 2(c). The radial stub and the QWML can be cascaded to achieve sufficient frequency bandwidth [18], [20]. Two radial stubs biasing network with QWML is shown in Figure 2(d). The disadvantage of this technique is in the tremendous increase of the size of the circuit as compared to the increase of the bandwidth. Research has shown that with only a single radial stub biasing network, both broad bandwidth and compact circuit size can be also be achieved. The advantage of a single radial stub biasing network is that the reduction of the circuit dimension is 50% as compared to the cascaded double radial stub resonator.

Xuan *et al.* [21] have designed the concurrent multiband biasing network with the quarter-wave transmission line and quarter-wave open circuit stub (QWOS) shown in Figure 2(e). For the first band corresponding to the centre frequency of  $f_1$ , the QWOS will create a short at point 1 on the main transmission line. The main transmission line with a length  $l_1$ , equivalent to the  $\lambda/4$  at the centre frequency, will convert the short circuit into an open circuit. The same argument is applied to the other frequency band. For the 2<sup>nd</sup> band, the quarter wavelength line corresponding to the centre frequency is calculated and then adjusted step by step in the same manner. Here, the convention  $f_1 > f_2 \dots > f_n$  is used. Multiband biasing network works better at the certain frequency band but in the middle of the bands, the performances are very poor. For this reason, the multiband biasing network cannot be used for wideband RFPA. The new biasing network which is suitable for the wideband RFPA is described in the following research methodology section.

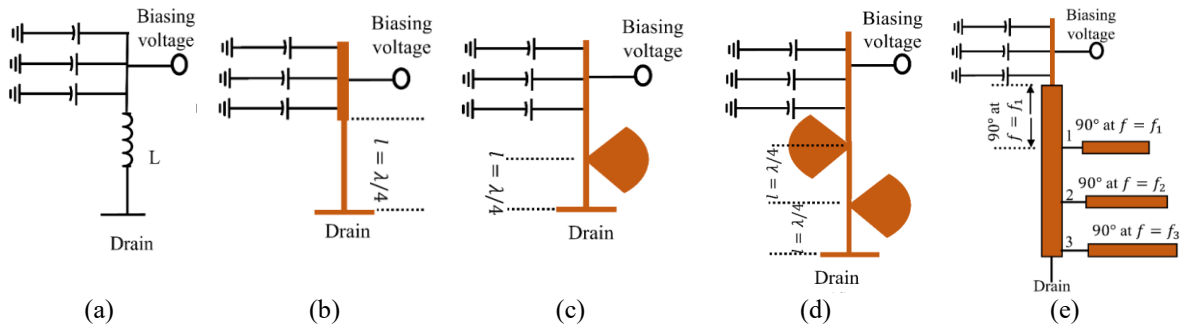


Figure 2. Different types of biasing network: (a) using a wideband biasing choke, (b) using a quarter-wave transmission line, (c) using a quarter-wave transmission line and radial stub, (d) cascading the quarter-wave transmission line and radial stub and (e) connecting the multiple frequencies open circuit stub and quarter wave transmission line

### 3. DESIGN OF THE BIASING NETWORK

The ideal biasing network works as an open circuit at the desired RF bandwidth and short circuit at DC. But in practice, it is not possible to maintain perfect isolation from the DC voltage for the whole bandwidth. Therefore, the biasing network is designed in such a way that it maintains standard isolation (minimum 30dB) from the DC sources. For ease, the biasing network is designed considering the centre frequency of the band. The frequency band for this research is from 3.3 to 4.3 GHz, and the centre frequency is 3.8 GHz. To achieve a wider band stop, the width of the QWML should be as narrow as possible. In other words, the characteristic impedances of the QWML line should be as high as possible. In practice, the possible line width is limited by the fabrication tolerance and the DC current handling capacity of the laminate [20]. The fabrication tolerance of the computer numerical control (CNC) machine is 0.2mm, but in reality, it is not feasible. Therefore, the minimum width of the microstrip line is chosen 0.3mm. The input impedance of the transmission line is given by the (1) [22].

$$Z_i(l) = Z_0 \frac{Z_L + jZ_0 \tan \beta l}{Z_0 + jZ_L \tan \beta l} \quad (1)$$

Where,  $Z_L$  and  $Z_o$  are the load impedance and the characteristic impedance of the transmission line, respectively.  $\beta l$  is the electrical length of the transmission line. If  $Z_L = 0$ , i.e. the load is short-circuited at the load point, then the input impedance of the transmission line is given by the  $Z_{in}^S = jZ_o \tan \beta l$ . On the other hand, if  $Z_L = \infty$ , i.e. open-circuited at the load point, then the input impedance of the transmission line is given by  $Z_{in}^O = -jZ_o \cot \beta l$ . If the transmission line is precisely quarter-wave, then the (4) reduces to  $Z_i = \frac{Z_o^2}{Z_L}$ . This means the input impedance is inversely proportional to the load impedance. Therefore, the quarter-wave transmission line transforms a short-circuit into an open-circuit and vice versa.

First of all, the biasing network is simulated using the Keysight Advanced Design System (ADS) at the schematic window. The basic biasing network is designed using the QWOS and the quarter-wave transmission line (QWTL) at the centre frequency, as shown in Figure 3(a) and corresponding input impedance response is shown in Figure 3(b). The QWOS converts the open to the short-circuit, and the QWTL converts the short to the open at the drain. In practice, the open circuit stub transfers an infinite impedance to a low complex impedance, and the low complex impedance is converted into a high complex impedance. But the high complex impedance is converted to a medium complex impedance. For this reason, at the frequency of the second harmonic (7.6 GHz), it shows a high impedance value instead of a zero impedance at the drain. Then, the ideal transmission line is converted to a microstrip line using the RO3006C substrate. The properties of the substrate are given in Table 1.

Table 1. Rogers RO3006 substrate characteristics

Parameters	Value
Relative dielectric constant	6.15
Substrate thickness	1.27 mm
Conductor thickness	17.5 $\mu$ m
Dielectric loss tangent	0.002

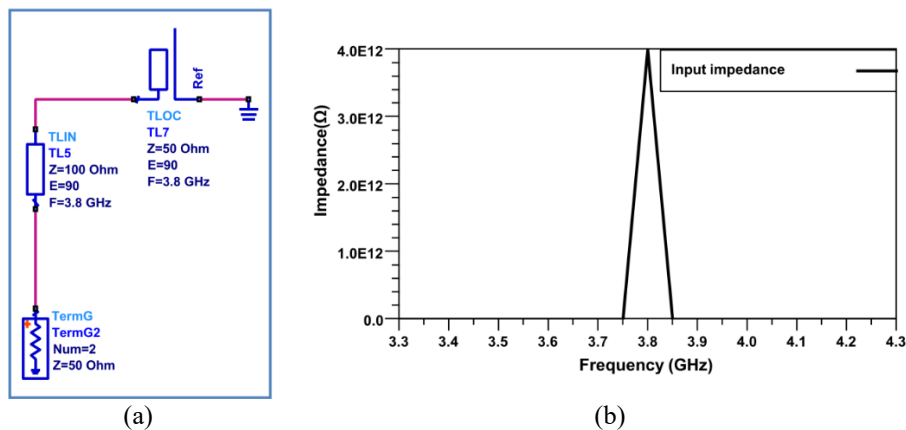


Figure 3. (a) Biasing network using the ideal transmission line and (b) The input impedance response

The converted biasing network with the microstrip line is shown in Figure 4(a) and the input impedance response is shown in Figure 4(b). From the Figure 4(b), it is seen that at the centre frequency, it offers a high impedance buffer but at the side of the band, it offers a low impedance buffer. Therefore, this arrangement is not suitable for the wideband power amplifier. To improve the performances, point A must be short-circuited through QWOS for the wideband, as shown in Figure 4(a). To achieve low impedance at point A, the characteristic impedance of the QWOS must be decreased which results in an increase in the width of the line. At point B, to get a high impedance buffer, the characteristic impedance of QWML must be as high as possible which reduces the width of the line. The QWML and the shunt of QWOS must be connected through a microstrip T-junction (MTEE). For the MTEE, the ratio of the largest width to the smallest width must be less than 5. Otherwise, the schematic and momentum simulation performance will not be the same. Another problem of a straight stub is that at the high frequency, the width of the low characteristic impedance microstrip line will be a fraction of the wavelength which in turn causes an excitation of the unwanted signal mode [18]. These two problems can be solved by replacing an open-circuit stub with a radial stub. A radial stub offers a better short circuit for a wide frequency band as compared to a straight stub. Better performances can be achieved due to the fringing capacitance effect at the end of the radial stub [23], and it does not suffer a large width tee junction that a constant-width low-impedance stub would.

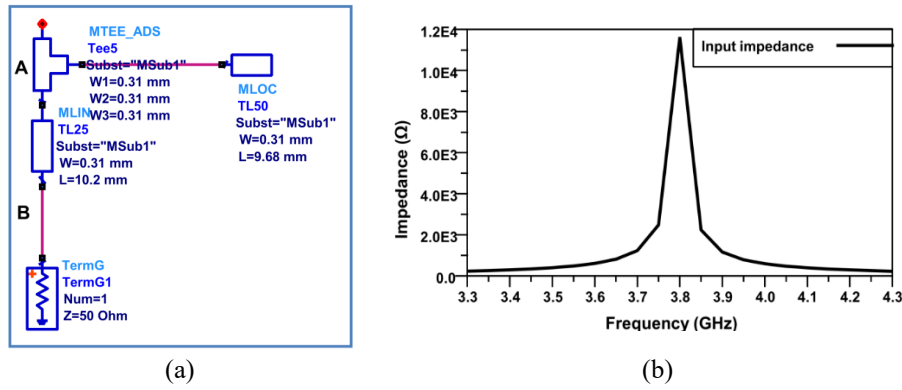


Figure 4. (a) Biasing network with microstrip line and (b) The input impedance response

The performances of the butterfly stub are somewhat better as compared to the radial stub. It provides virtual ground for wideband than radial stub [24], [25]. For this reason, a butterfly stub is used for the design of the biasing network. The parameter of the butterfly stub is calculated based on the centre frequency of 3.8 GHz of the band. The outer radius  $r_o$  determines the attenuation pole frequency whereas the angle determines the attenuation bandwidth [20]. It is clear that a larger radius results in a lower attenuation pole frequency. It is also seen that if the angle of the radial stub is increased then the reactance slope of the input reactance of the radial stub is decreased and, as a result, the bandwidth of attenuation is increased. The input width  $w_i$  of the port has the small effect on both attenuation pole and frequency bandwidth. The input width should be small compared to the guided wavelength. Generally, the input width should be the same as the connective inductive width length.

A wideband RF bypass at the drain bias is essential to boost up the performance of the biasing network [4]. The broadband RF bypass includes a combination of the different valued capacitor. Generally, picofarad, nanofarad, and microfarad capacitor are connected at the drain bias. The picofarad capacitor provides low impedance at high frequency at the same time the other two capacitors provide low impedance at medium and low frequency. So, to provide the soldering space for the capacitor and the DC supply, another wide microstrip line is needed which will not affect the performances of the biasing network. Therefore, another microstrip line is added to the biasing circuit. The complete schematic circuit diagram is shown in Figure 5(a). After that, the layout is created from the schematic design, as shown in Figure 5(b), and the microwave momentum simulation is performed. The final values of the dimension are shown in Table 2. After the biasing network is fabricated, as shown in Figure 6, the S-parameter of the biasing network is measured as shown in Figure 7 using the Rohde & Schwarz VNA, model ZNB8.

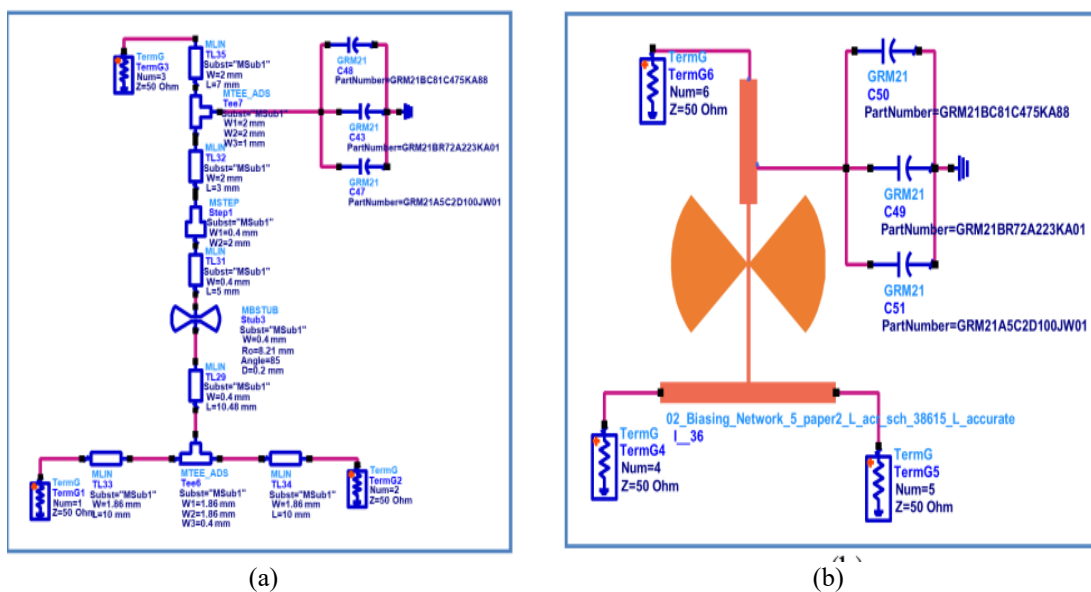


Figure 5. Complete biasing network (a) schematic simulation and (b) momentum simulation

Table 2. Calculated parameters of the biasing network and after the optimization

Name	Calculated (mm)	Optimized (mm)
Width of feed line $w$	0.40	0.4
Outer radius $R_o$	8.21	9
Angle	85	85
Insertion depth $D$	0.2	0.2
TL29	W=0.4, L= 10.48	W=0.4, L= 10.2
TL33	W=1.86, L= 10	W=1.86, L=10
TL34	W=1.8, L= 10	W=1.86, L=10
Biasing Capacitors	10 pF, 22 nF, 4.7 uF	10 pF, 22 nF, 4.7 uF

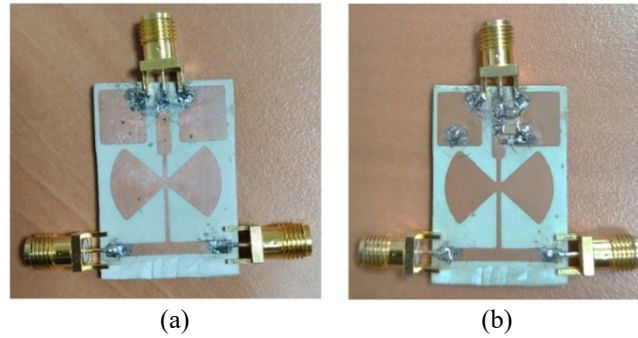


Figure 6. Fabricated biasing network (a) without bypass capacitor and (b) with bypass capacitor

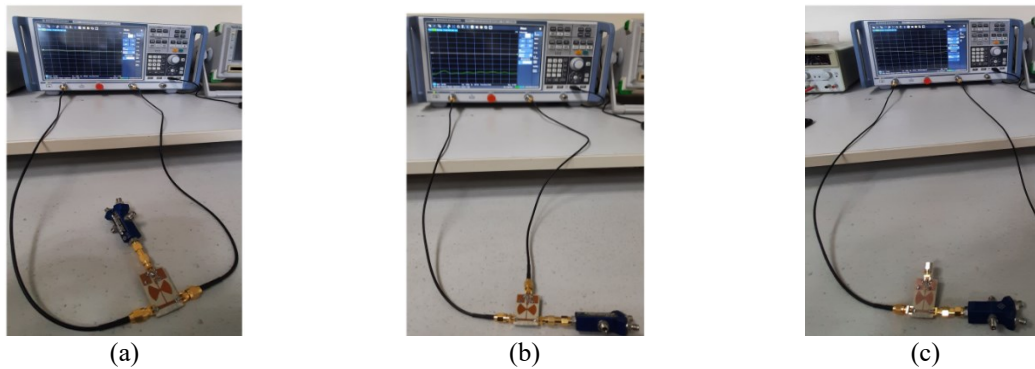


Figure 7. Measurement of (a)  $S_{21}$ , (b)  $S_{31}$  and (c)  $S_{11}$

#### 4. RESULTS AND ANALYSIS

The performances of the biasing network are determined in terms of three critical parameters: the transmission gain  $S_{21}$ , the return loss  $S_{11}$  and the RF isolation  $S_{31}$ . Low transmission gain and high return loss could reduce the RF power dissipation in the biasing circuit. The RF isolation to the DC input port should be as high as possible but must reach a minimum of 30 dB. It can prevent the oscillation of the PA. The simulation and fabricated performances are shown in Figure 8(a), 8(b) and 8(c). The performance of the biasing network in term of the transmission gain,  $S_{21}$  is very good over the whole frequency band, as shown in Figure 8(a). In the simulation, the values of  $S_{21}$  is in the range of 0 to 0.2 dB, but for the fabricated circuit, it is in the range of 0.0 dB to 1.5 dB for which it is very low as compared to the other type of biasing network. From Figure 8(b), it is seen that the return loss  $S_{11}$  of the fabricated circuit is in the range between 9 dB and 19 dB and maximum at the frequency of 3.9 GHz while in simulation, the value is from 25 dB to 50 dB. The measured performances vary substantially from the simulation due to the accuracy of the fabrication. For the narrow transmission line, it is very difficult to maintain the consistency with the etching procedure.

Figure 8(c) shows the RF isolation to DC connection,  $S_{31}$  simulated and measured results of the biasing network. The simulated result is in the range between 37 dB to 65 dB while for the fabricated biasing network, it is in the range of 35 to 45 dB after connecting the bypass capacitor. The RF isolation performance is improved a little bit after connecting the capacitor. The schematic and measured performances of  $S_{31}$  is comparable with acceptable accuracy. The RF isolation depends on the value of the capacitor. For this design, the capacitor 10 pF, 22 nF and 4.7 uF for the low, medium and high-frequency bypass. The designed biasing network is compared to the state-of-

the-art biasing network as shown in Table 3. From the table, it is seen that the designed biasing network provides the highest RF isolation to the DC while it is comparable for the other parameters.

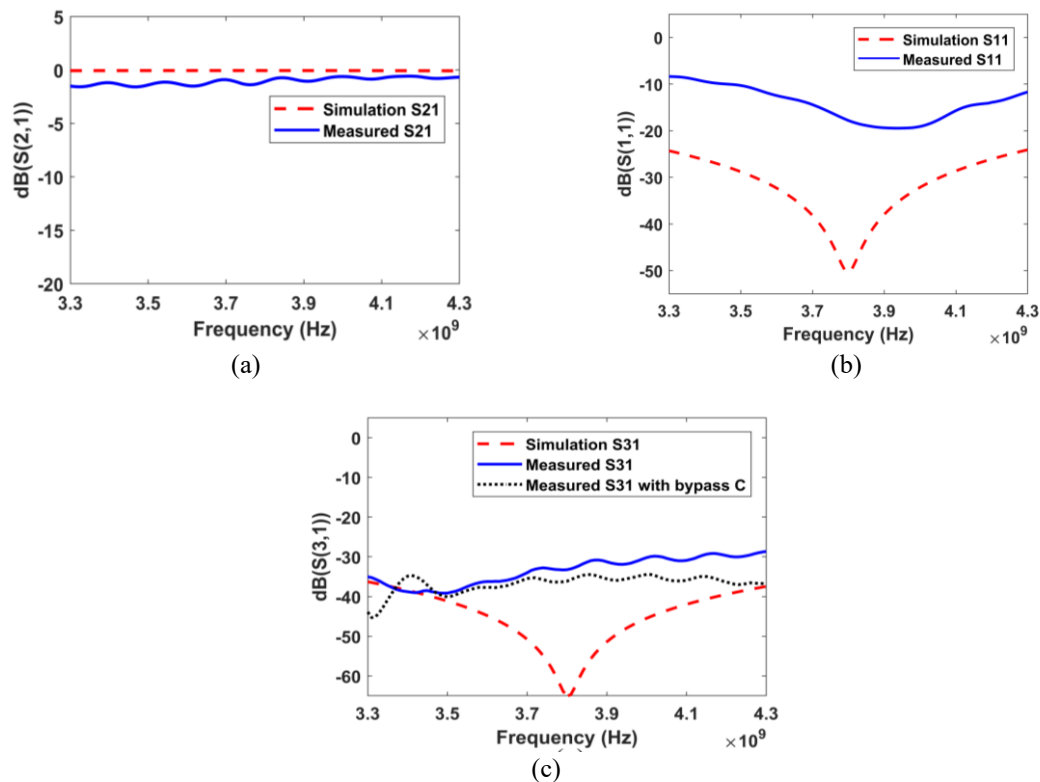


Figure 8. Performances of biasing network in simulation and fabricated circuit (a) transmission gain  $S_{21}$  (b) return loss  $S_{11}$  and (c) RF isolation  $S_{31}$  without and without bypass capacitor

Table 3. Comparison with the state-of-the-art

Ref	Frequency (GHz)	$S_{11}$ (dB)	$S_{21}$ (dB)	$S_{31}$ (dB)	Result type
[8]	7-9	< 20	< 0.4	< 30	Fabricated
[17]	3.1-10	25-35	<0.3	n/m	Simulation
[19]	7-8	n/m	<0.5	n/m	Simulation
[24]	3.1-4.8	12-45	<0.4	n/m	Simulation
This work	3.3-4.3	9-19	<1.5	35-45	Fabricated

n/m: not mentioned

## 5. CONCLUSION

The efficient communication system requires highly efficient RFPA. The wideband biasing network is mandatory for high efficiency RFPA. So, a wideband biasing is presented in this paper which can be implemented for the 5G frequency band of 3.3 GHz to 4.3 GHz. Not only for this band but also for any frequency band, this technique of designing biasing can be applied. The fabricated biasing network provides 9 to 19 dB return loss, 35 to 45 dB RF isolation, and 0.5 to 1.5 dB insertion loss. In future, the RFPA power amplifier will be designed for the mentioned frequency band using this biasing technique, and it is expected that it will perform better for the 5G communication system.

## ACKNOWLEDGEMENTS

The authors would like to acknowledge the MMU-GRA fund MMUI/180270.02 from Multimedia University and the FRGS fund FRGS/1/2019/TK04/MMU/02/15 from the Ministry of Higher Education Malaysia (MOHE) for funding this research activity. The authors also would like to thank Kumpulan Kabex Sdn Bhd and Rohde & Schwarz for providing the Vector Network Analyzer (R&S ZNB8) for the measurement.

## REFERENCES

- [1] S. Y. Zheng, Z. W. Liu, X. Y. Zhang, X. Y. Zhou, and W. S. Chan, "Design of Ultrawideband High-Efficiency Extended Continuous Class-F Power Amplifier," *IEEE Trans. Ind. Electron.*, vol. 65, no. 6, pp. 4661-4669, Jun. 2018, doi: 10.1109/TIE.2017.2772163.
- [2] P. Saad, C. Fager, H. M. Nemati, H. Cao, H. Zirath, and K. Andersson, "A Highly Efficient 3.5 GHz Inverse Class-F GaN HEMT Power Amplifier," *Int. J. Microw. Wirel. Technol.*, vol. 2, no. 3-4, pp. 317-324, 2010, doi: 10.1017/S1759078710000395.
- [3] B. Battaglia, "The ABCs of Device Biasing," *Microwave Journal*, vol. 43, no. 11, p. 136, 2000.
- [4] O. Ceylan, S. Pires, and L. Marco-Platon, "Refine Biasing Networks for High PA Low-Frequency Stability," *Microwaves RF*, vol. 57, pp. 52-56, 2018, Accessed: Dec. 20, 2019. [Online]. Available: <https://www.mwrf.com/technologies/systems/article/21849097/refine-biasing-networks-for-high-pa-lowfrequency-stability>
- [5] M. Iqbal, "Advanced High Efficiency and Broadband Power Amplifiers Based on GaN HEMT for Wireless Applications," *Politecnico Di Torino*, 2017, doi: 10.6092/polito/porto/2672421.
- [6] Z. Yang, Y. Yao, Z. Liu, M. Li, T. Li, and Z. Dai, "Design of High Efficiency Broadband Continuous Class-F Power Amplifier Using Real Frequency Technique with Finite Transmission Zero," *IEEE Access*, vol. 6, pp. 61983-61993, 2018, doi: 10.1109/ACCESS.2018.2875010.
- [7] A. B. Stenström, "Wideband Efficiency in a Class-F Power Amplifier," *Master's thesis*, Norwegian University of Science and Technology, 2014.
- [8] Y. W. Yeap, L. H. Chua, and S. H. Tan, "Design of 12W X-Band High Power Cascade Amplifier," *2004 RF Microw. Conf. RFM 2004 - Proc.*, no. April, pp. 9-12, 2004, doi: 10.1109/rfm.2004.1411060.
- [9] G. Ancans, V. Bobrovs, A. Ancans, and D. Kalibatiene, "Spectrum Considerations for 5G Mobile Communication Systems," *Procedia Comput. Sci.*, vol. 104, no. December 2016, pp. 509-516, 2016, doi: 10.1016/j.procs.2017.01.166.
- [10] E. Team, "5G Frequency Bands," 2018. Accessed: Aug. 19, 2019. [Online]. Available: <https://www.everythingrf.com/community/5g-frequency-bands>
- [11] M. G. Sadeque, Z. Yusoff, and M. Roslee, "A High-Efficiency Continuous Class-F Power Amplifier Design using Simplified Real Frequency Technique," *Bull. Electr. Eng. Informatics*, vol. 9, no. 5, pp. 1924-1932, 2020, doi: 10.11591/eei.v9i5.2227.
- [12] "Methods of Transistor Biasing - Tutorialspoint," Accessed: July 20, 2020. [Online]. Available: [https://www.tutorialspoint.com/amplifiers/methods\\_of\\_transistor\\_biasing.htm](https://www.tutorialspoint.com/amplifiers/methods_of_transistor_biasing.htm)
- [13] M. R. Rahman, "Class E GaN Power Amplifier Design for WiMAX Base Stations," *University of Ottawa*, 2016.
- [14] C. Yu, B. Zhang, J. Gao, Y. Liu, H. Huang, and Y. Wu, "Design of Multioctave Bandwidth Power Amplifier Based on Resistive Second-Harmonic Impedance Continuous Class-F," *IEEE Microw. Wirel. Components Lett.*, vol. 27, no. 9, pp. 830-832, 2017, doi: 10.1109/lmwc.2017.2734764.
- [15] G. Liu, F. Mu, X. Qiu, Y. Leng, and X. Peng, "Design of Broadband Power Amplifier Based on Continuous Class-F Mode with Frequency Parameterization," *IEICE Electron. Express*, vol. 16, no. 6, pp. 1-4, 2019, doi: 10.1587/elex.16.20190038.
- [16] A. Rachakh, L. El Abdellaoui, J. Zbitou, A. Errkik, A. Tajmouati, and M. Latrach, "A Two-stages Microstrip Power Amplifier for WiMAX Applications," *TELKOMNIKA (Telecommunication Comput. Electron. Control)*, vol. 16, no. 6, pp. 2500-2506, 2018, doi: 10.12928/TELKOMNIKA.v16i6.9338.
- [17] N. T. Kim, "Ultra Wideband Bias Tee Design using Distributed Network Synthesis," *IEICE Electron. Express*, vol. 10, no. 15, pp. 1-8, 2013, doi: 10.1587/elex.10.20130472.
- [18] R. Dehbashi, H. D. Oskouei, and K. Forooraghi, "A Novel Broad-Band Microstrip Radial Stub Resonator Used in Bias-T Application," *Microw. Opt. Technol. Lett.*, vol. 48, no. 09, pp. 1766-1770, 2006, doi: 10.1002/mop.
- [19] R. M. A. Khan and S. Zaheer, "Design and Implementation of a 7-8 GHz Low-Noise Amplifier," *Linköping University*, 2012.
- [20] J.-S. Hong, "Microstrip Filters for RF/Microwave Applications," *Second Edi. A John Wiley & Sons, Inc*, 2011, doi: 10.1002/0471221619.
- [21] A. N. Xuan and R. Negra, "Design of Concurrent Multiband Biasing networks for Multiband RF Power Amplifiers," *42nd Eur. Microw. Conf.*, 2012, pp. 1-4, doi: 10.23919/eumc.2012.6459311.
- [22] D. M. Pozar, "Microwave Engineering," *4th ed. John Wiley & Sons, Inc*, 2011.
- [23] K. S. Tsang, "Class-F Power Amplifier with Maximized PAE," *California Polytechnic State University*, 2010.
- [24] E. Ottosson, "Design and Implementation of a Ultra Wide-band and Low-noise Amplifier 3.1-4.8 GHz," *Linköping University*, 2006.
- [25] N. S. R. Hadi, Z. Yusoff, M. G. Sadeque, S. J. Hashim, and M. A. Chaudhary, "High Gain over an Octave Bandwidth Class-F RF Power Amplifier Design using 10w GaN HEMT," *Bull. Electr. Eng. Informatics*, vol. 9, no. 5, pp. 1899-1906, 2020, doi: 10.11591/eei.v9i5.2226.



## BIOGRAPHIES OF AUTHORS



**Md. Golam Sadeque** has received B. Sc. Eng. degree in Electrical and Electronics Engineering (EEE) from Rajshahi University of Engineering and Technology (RUET) in 2011. He is pursuing a master of engineering science (M. Eng. Sc.) degree under the faculty of engineering at Multimedia University. He is also working as a lecturer since 23 June 2013 (now on study leave) in the department of EEE at Pabna University of Science and Technology (PUST), Pabna-6600, Bangladesh. His research interest includes the design of Radiofrequency power amplifier (RFPA) and Biomedical engineering. E-mail: golamsadeq@gmail.com



**Dr. Zubaida Yusoff** holds the position of a Senior Lecturer at the Faculty of Engineering, Multimedia University. She received her B.Sc. in Electrical and Computer Engineering (cum laude with distinction) and M.Sc. in Electrical Engineering from The Ohio State University, USA in 2000 and 2002 respectively. She worked with Telekom Malaysia International Network Operation in 2002 before she joined Multimedia University in 2004. She continued her studies at Cardiff University, Wales, UK in 2008 and received Ph. D degree in 2012. Dr Zubaida has presented technical papers at conference nationally and internationally. One of her conference papers has received "Honorable Mention" for the Student Paper Competition at the International Microwave Symposium, USA in 2011. She has authored/co-authored more than 25 journals and conference papers. Her teaching and research focus in the area of Microelectronics, Analog/Mixed Signal RF Circuit Design and Microwave/mm-wave Power Amplifier System.



**Associate Professor Dr. Mardeni Roslee** is an academician under Faculty of Engineering, Multimedia University, Cyberjaya, Malaysia. At Multimedia University, he is a current Deputy Director of Research Institute of Digital Connectivity, Chair of Centre of Wireless Technology and Chief Executive Officer (CEO) and Founder of Armada company. He serves as current Chair of IEEE Malaysia Comsoc/VTS, which is for recognized and selected members in professional organization, networking and interaction with like-minded multidisciplinary professionals. His current research interests are 5G/6G telecommunication, D2D, satellite, Internet of Things and radar communication. He has published over 90 indexed international journals and conference papers. He has 34 completed PhD and Masters and 10 on-going postgraduate students. He has awarded various international/local awards including being awarded the University Excellent Researcher Award for 2016 and 2018, respectively.



**Dr. Shaiful J. Hashim** is currently an Associate Professor in the Department of Computer and Communication Systems Engineering, Faculty of Engineering, Universiti Putra Malaysia (UPM). He received his Ph. D from Cardiff University, UK (2011), M. Sc from National University of Malaysia (2003) and B.Eng. from University of Birmingham, UK (1998) in the field of Electrical and Electronics Engineering. His research interests include cloud computing, Internet of Things (IoT), network security and non-linear wireless measurement system.



**Azah Syafiah** is a professional engineer (P.Eng) and a researcher at TM R&D Sdn Bhd since 2002. She holds a BEng (Hons) in Electronics from Multimedia University, Cyberjaya (2002) and MSc in Communications Engineering from Durham University, UK (2008). She has 18 years of experience in wireless technology research mainly in RF, Microwave and Mm-wave module and transceiver design, testing and development. Her recent interest is connectivity solutions for high-speed Internet. She is a IEEE senior member and also served as executive committee for IEEE Malaysia section (2019) and IEEE Malaysia Joint Chapter AP/MTT/EMC.